Macromolecules

Article

pubs.acs.org/Macromolecules

Photo-Induced Ligation of Acrylonitrile-Butadiene Rubber: Selective Tetrazole–Ene Coupling of Chain-End-Functionalized Copolymers of 1,3-Butadiene

Christoph J. Dürr,[†,‡] Paul Lederhose,[†,‡] Lebohang Hlalele,[†,‡] Doris Abt,[†,‡] Andreas Kaiser,[§] Sven Brandau,[§] and Christopher Barner-Kowollik*[,†,‡]

[†]Preparative Macromolecular Chemistry, Institut für Technische Chemie und Polymerchemie, Karlsruhe Institute of Technology (KIT), Engesserstrasse 18, 76128 Karlsruhe, Germany

[‡]Institut für Biologische Grenzflächen, Karlsruhe Institute of Technology (KIT), Hermann-von-Helmholtz Platz 1, 76344 Eggenstein-Leopoldshafen, Germany

[§]Lanxess Emulsion Rubber, BP 7–Z.I. Rue du Ried, 67610 La Wantzenau, France

Supporting Information

ABSTRACT: A highly selective photo-induced nitrile imine mediated tetrazole–ene coupling (NITEC) of chain-end-functionalized nitrile–butadiene rubber (NBR) is reported, providing nitrile rubbers with molar masses of up to 48 000 g·mol^{-1}. NBR was obtained via the reversible addition–fragmentation chain transfer (RAFT) mediated copolymerization of acrylonitrile and 1,3-butadiene employing a novel photoreactive tetrazole-functionalized trithiocarbonate. The herein reported tetrazole-functionalized trithiocarbonate represents—to the best of our knowledge—the first ever reported photoreactive RAFT agent capable of undergoing light-induced ligations with enes. Molar masses of the tetrazole-functionalized NBRs were in the range of 1000 to 38 000 g·mol^{-1} with dispersities between 1.1 to 1.6. By an appropriate choice of the tetrazole substituents, a reaction of the *in situ* formed enophile with the double bonds or the nitrile moieties of the incorporated monomer units within the polymer backbone—present in high excess relative to the dipolarophile linker molecule—was not observed. Underpinned by DFT calculations, the selectivity was identified to originate from a reduced LUMO energy level of the maleimide linker compared to the nonactivated backbone olefins when employing a nitrile–imine of moderate reactivity.

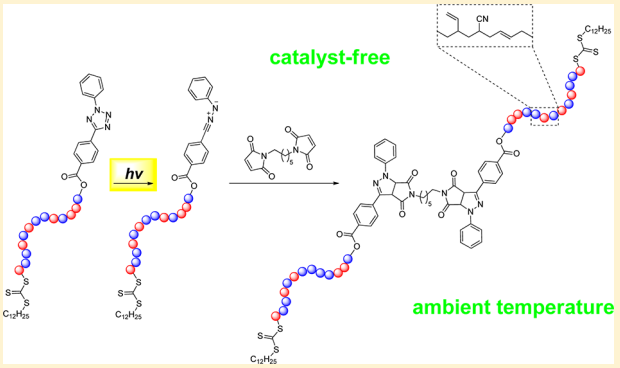

INTRODUCTION

Within the past decade, orthogonal ligation techniques have found substantial interest in the field of polymer chemistry.[1−4] Their advent originates from the introduction of reversible-deactivation polymerization techniques such as nitroxide mediated polymerization (NMP),[5] atom transfer radical polymerization (ATRP)[6] and reversible addition–fragmentation chain transfer (RAFT) polymerization[7−12] allowing the synthesis of polymers with well-defined chain-end functionality.[13] Orthogonal ligation is applied in all fields of modern polymer science[2,14] and has been employed for chain-end functionalization, dendrimer-,[15,16] block- and star (co)-polymer[17] synthesis and the immobilization of polymers on solid (bio)substrates.[18,19] The most prominent ligation technique, the copper mediated azide–alkyne cycloaddition (CuAAC), was reinvented by Kolb, Finn, and Sharpless[20] with the introduction of the "click" concept in 2001 and since then continuously refined. In recent years, strategies to improve catalysts in efficiency[21] and nature[22] were developed and catalyst-free strategies employing ring-strained cycloalkynes[23] were proposed. In addition, several other thermally,[24,25] chemically[26−29] or photochemically[30−34] triggered ligation protocols have been developed. An outstanding example of an orthogonal ligation chemistry is the UV-light triggered nitrile imine mediated tetrazole–ene coupling (NITEC).[35−38] First described in 1967 by Huisgen and co-workers,[39] the method is mainly applied in the field of biochemistry[40−42] and was used for bio-orthogonal conjugation of proteins in vitro[43] and in vivo.[44,45] Recently, polymer scientists have found interest in this technique free of catalysts and additives for the modification of polymersomes[46] or the spatially controlled immobilization of polymers on silicon or cellulose.[47] Mechanistically, the irreversible light triggered release of molecular nitrogen from a 2,5-tetrazole provides a nitrile imine dipole that reacts *in situ* with olefins—either activated or unactivated—via the formation of a pyrazoline structure.

Received: June 4, 2013
Revised: June 27, 2013

   dx.doi.org/10.1021/ma401154k | *Macromolecules* XXXX, XXX, XXX–XXX

Scheme 1. Overall Strategy of the UV-Induced Modular Coupling of NBR Building Blocks to Obtain High Molecular Weight Nitrile Rubber

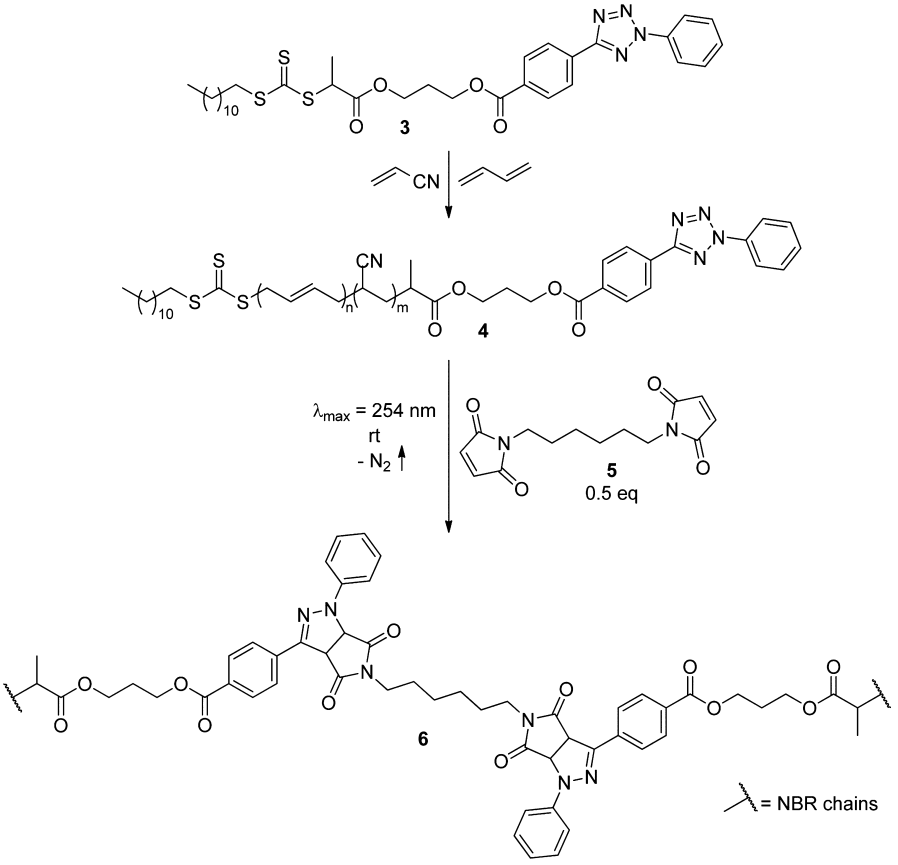

We recently reported the reversible-deactivation radical copolymerization of acrylonitrile (AN) and 1,3-butadiene (BD) to obtain nitrile–butadiene rubber (NBR) of low dispersity under controlled molecular weight conditions.[48,49] The RAFT polymerization protocol was further exploited for the utilization of chain-end functionality in successive modular strategies for the synthesis of block- and miktoarm star copolymers via hetero-Diels–Alder cyclizations[50] and—by employing a CuAAC reaction pathway—for the accessibility of molar masses above those that can be obtained in sequential RAFT polymerizations.[48,51]

In the current contribution, a photo-induced approach for the synthesis of linear high molecular weight acrylonitrile–butadiene rubber (NBR) via the NITEC is presented. Such an approach is highly desirable, since linear high molecular weight polymer of the technically important synthetic rubber cannot be obtained in a sequential RAFT process. With respect to an industrial application, the NITEC technique overcomes the limitations of other ligation techniques derived from the need of metal catalysts, often exhibiting negative effects on NBR aging properties.[52] The presented photochemical tetrazole–ene coupling technique reveals a high selectivity and solely proceeds with the specific linker molecule. A coupling of the tetrazole chain-ends with the "enes" present in high concentrations within the NBR backbone is not observed.

Our overall strategy of NBR coupling is depicted in Scheme 1. A novel tetrazole-functionalized controlling agent **3**—representing, to the best of our knowledge, the first ever reported photoreactive tetrazole-functionalized RAFT agent capable of undergoing light-induced ligations with enes—was synthesized from 4-(2-phenyl-2*H*-tetrazol-5-yl)benzoic acid (**2**) in two consecutive esterification steps and employed in the RAFT mediated radical copolymerization of AN and BD. In the presence of a small molecule linker, bis(maleimido)hexane (**5**), the RAFT based photoreactive polymers (**4**) were irradiated with UV-light (λ_{max} = 254 nm) to form the diaryl nitrile imine enophile *in situ*. The nitrile imine and the dipolarophile maleimide subsequently react to give the coupled NBR (**6**).

EXPERIMENTAL SECTION

Materials. Acrylonitrile (AN, > 99%, Acros), 1,3-butadiene (BD, > 99.5%, Air Liquide), *N*,*N*′-dicyclohexylcarbodiimide (DCC, 99%, Acros), 4-(dimethylamino)pyridine (DMAP, 99%, Aldrich), propane-1,3-diol (98%, Aldrich), benzenesulfonyl hydrazide (98%, ABCR), 4-formylbenzoic acid (97%, Aldrich), acetonitrile (Rotisolv, HPLC grade), pyridine, (99%, ABCR), aniline (>99.5%, Aldrich), sodium nitrite (97+%, Acros), hydrochloric acid (37%, Roth), 1,1′-azobis-(cyclohexane-1-carbonitrile) (98%, Aldrich), 1-ethylpiperidine hypophosphite (95%, Aldrich), 1-octene (98%, Aldrich), *trans*-3-octene (97%, ABCR) and chlorobenzene (Acros, 99+%) were used without further purification. 1,6-Bis(maleimido)hexane (**5**) was obtained from BASF SE, Ludwigshafen, Germany. Other solvents (synthesis grade) were obtained from VWR and used as received. 2-((Dodecylsulfanyl)-carbonothioyl)sulfanyl propanoic acid (DoPAT) was obtained from Lanxess Deutschland GmbH. 4-(2-Phenyl-2*H*-tetrazol-5-yl)benzoic acid was synthesized according to the literature.[35]

Synthesis of Tetrazole-Functional RAFT Agent (3). DoPAT (2.000 g, 5.7 mmol), DMAP (0.014 g, 0.1 mmol), and 1,3-propanediol (1.299 g, 17.1 mmol) were dissolved in 10 mL of THF. The solution was cooled to 0 °C and DCC (1.290 g, 6.3 mmol) was added. The cooling bath was removed and the reaction mixture was stirred at ambient temperature for 16 h. THF was removed under reduced

dx.doi.org/10.1021/ma401154k | *Macromolecules* XXXX, XXX, XXX–XXX

pressure. The obtained solid was dissolved in Et_2O, extracted with 1 M hydrochloric acid (4 × 100 mL) and washed with saturated $NaHCO_3$ solution (100 mL). The organic layer was dried over $MgSO_4$ and Et_2O was removed under reduced pressure. The crude product was purified via column chromatography on silica gel using hexane/ethyl acetate (3:1, v/v, R_f 0.36) as the eluent. After drying under high vacuum compound **1** was obtained as a yellow oil (1.591 g, 68%).

^{1}H NMR (400 MHz, $CDCl_3$): δ 4.83 (q, J = 7.4 Hz, 1H, $CH(CH_3)$), 4.31−4.28 (m, 2H, C(O)O−CH_2), 3.69 (t, J = 7.4 Hz, 2H, CH_2−OH), 3.34 (t, J = 7.4 Hz, 2H, S−CH_2), 1.90−1.86 (m, 2H, O−CH_2−CH_2−CH_2−OH), 1.70−1.66 (m, 2H, S−CH_2−CH_2), 1.59 (d, J = 7.4 Hz, 3H, $CH(CH_3)$), 1.42−1.38 (m, 2H, S−CH_2−CH_2−CH_2), 1.26−1.21 (m, 16H, CH_3−$(CH_2)_8$), 0.86 (t, J = 7.4 Hz, 3H, CH_2−CH_3).

^{13}C NMR (101 MHz, $CDCl_3$): δ 222.27 (C(S)−S), 171.28 (C(O)−O), 62.00, 48.16, 37.37, 32.05, 29.76, 29.75, 29.68, 29.56, 29.47, 29.22, 29.03, 28.02, 22.82, 17.09, 14.25, 14.22 (CH_2−CH_3).

The hydroxyl-functional RAFT agent **1** (3.800 g, 9.3 mmol), DMAP (0.026 g, 0.02 mmol) and diaryl tetrazole **2** (2.890 g, 10.9 mmol) were dissolved in 20 mL THF. The solution was cooled to 0 °C and DCC (2.450 g, 11.9 mmol) was added. After stirring the reaction mixture for 16 h at ambient temperature THF was removed under reduced pressure. The obtained solid was dissolved in Et_2O, extracted with 1 M hydrochloric acid (4 × 200 mL) and washed with saturated $NaHCO_3$ solution (200 mL). The organic layer was dried over $MgSO_4$ and Et_2O was removed under reduced pressure. The crude product was purified via column chromatography on silica gel using hexane/ethyl acetate (3:1, v/v R_f 0.47) as the eluent. After drying under high vacuum the title compound **3** was obtained as a yellow oil (2.760 g, 45%).

^{1}H NMR (400 MHz, $CDCl_3$): δ 8.28 (d, J = 7.6 Hz, 2H, H_d), 8.17−8.10 (m, 4H, $H_{d',c}$), 7.53 (t, J = 7.3 Hz, 2H, C_6H_5-*meta*-H), 7.46 (t J = 7.4 Hz, 1H, C_6H_5-*para*-H), 4.81 (q, J = 7.1 Hz, 1H, $CH(CH_3)$), 4.45 (t, J = 7.9 Hz, 2H, aryl−C(O)O−CH_2), 4.33 (t, J = 6.8 Hz, 2H, $CH(CH_3)$−C(O)O−CH_2), 3.32 (t, J = 7.2 Hz, 2H, S−CH_2), 2.19−2.16 (m, 2H, O−CH_2−CH_2−CH_2−O), 1.66−1.60 (m, J = 7.1 Hz, 2H, S−CH_2−CH_2), 1.59 (d, J = 7.2 Hz, 3H, $CH(CH_3)$), 1.38−1.34 (m, 2H, S−CH_2−CH_2−CH_2), 1.38−1.33 (m, 16H, CH_3−$(CH_2)_8$), 0.86 (t, J = 7.2 Hz, 3H, CH_2−CH_3).

^{13}C NMR (101 MHz, $CDCl_3$): δ 222.19 (C(S)−S), 171.33 ($CH(CH_3)$−C(O)−O), 165.97 (aryl−C(O)−-O), 164.46 (C(N−R)−N), 136.92, 131.88, 131.47, 130.38, 130.03, 129.88, 127.14, 120.06, 62.55, 61.83, 47.96, 37.44, 32.04, 29.76, 29.74, 29.68, 29.57, 29.47, 29.22, 29.05, 28.12, 27.99, 22.82, 16.87, 14.25 (CH_2−CH_3).

Polymerizations. RAFT-mediated copolymerizations of AN and BD were performed in a pressure stable glass reactor in a setup described earlier.[48] Samples were taken after preset time intervals and precipitated in cold ethanol. Experimental details are provided in Table 2.

Coupling of Tetrazole-Functionalized NBR via NITEC. In a 50 mL round-bottom quartz glass flask, diaryl tetrazole-functionalized NBR was dissolved in acetonitrile. Then 0.5 equiv of bis(maleimido)-hexane linker was added from a stock solution in acetonitrile. The solution was irradiated with UV-light of 254 nm (Lamag TLC lamp, electric power 8 W, lamp-flask distance at the position of the largest flask diameter ∼5 cm) for 3 h. The solvent was removed under reduced pressure and the resulting polymers were analyzed without further purification.

DFT Calculations. The HOMO and LUMO energies were calculated using the B3LYP/6-31G//B3LYP/6-31G model chemistry with GAMESS.

Instrumentation. ^{1}H NMR and ^{13}C NMR spectra were recorded at ambient temperature on a Bruker Advance 400 NMR spectrometer or a Bruker AM 250 NMR spectrometer and referenced to the residual solvent signal.

Molecular weight determination was performed on a SEC system (PL-GPC 50 Plus, Polymer Laboratories) consisting of an auto injector, a guard column (PLgel Mixed C, 50 × 7.5 mm), three linear columns (PLgel Mixed C, 300 × 7.5 mm, 5 μm bead-size) and a differential refractive index detector using THF as the eluent at 35 °C and a flow rate of 1 mL·min^{-1}. The system was calibrated using narrow polystyrene standards (Polymer Standard Service) ranging from 160 to 6 × 10^6 g·mol^{-1}. Samples were injected from solutions in THF (2 mg·mL^{-1}) and molecular weight was evaluated with the Mark−Houwink−Kuhn−Sakurada parameters of NBR.[53]

ESI-MS spectra were recorded on a LXQ mass spectrometer (ThermoFisher Scientific, San Jose, CA) equipped with an atmospheric pressure ionization source operating in the nebulizer assisted electrospray mode. The system was calibrated with a standard containing caffeine, Met-Arg-Phe-Ala acetate, and a mixture of fluorinated phosphazenes (Ultramark 1621), purchased from Aldrich. A spray voltage of 4.5 kV, a dimensionless sweep gas flow rate of 2 and a dimensionless sheath gas flow-rate of 12 were applied. The capillary voltage, the tube lens offset voltage and the capillary temperature were set to 60 V, 110 V and 275 °C, respectively. For SEC−ESI−MS measurements the mass spectrometer was coupled to a Series 1200 HPLC-system (Agilent, Santa Clara, CA) with THF as the eluent in accordance to a setup described earlier.[54] Polymer samples were dissolved in THF at 2 mg·mL^{-1} and injected onto the HPLC system.

Fluorescence emission spectra were recorded in quartz cuvettes loaded with a sample volume of 230 μL on a Varian Cary Eclipse Fluorescence Spectrometer. UV absorption spectra were recorded on a Varian Cary 300 UV−vis spectrometer.

RESULTS AND DISCUSSION

Cyclization of various diaryl nitrile imines with nonactivated olefins was reported to proceed within seconds.[44] In NBR polymerizations, incorporation of BD into the growing polymer chain predominantly occurs in a 1,4-mode resulting in the formation of internal double bonds distributed along the polymer backbone. These double bonds are potential "dipolarophiles" able to react with the nitrile imine dipole. Close to 10% of the BD incorporation occurs in a 1,2-mode leading to pendant double bonds,[55] less sterically hindered and more readily available for cyclization than the internal ones. In 1972, Stille et al. investigated [4 + 2] cyclizations of nitrile imines and residual double bonds of styrene−butadiene type or natural rubber type elastomers for their thermally induced cross-linking.[56] In their work, tetrazole-functionalized styrene monomers were synthesized and copolymerized into the elastomers as pending nitrile imine dipole precursors. At elevated temperatures, cross-linked rubbers were obtained and characterized by solubility studies. Nitrogen release was observed at temperatures above 150 °C with tetrazole half-lives in the range of several minutes. Since the reaction kinetics and cyclization affinities of diaryl nitrile imines toward olefins strongly depend on the substitution patterns of the aromates, a careful choice of substituents on the aromatic rings of the diary tetrazole is crucial to prevent cross-linking of the tetrazole-functionalized NBRs and to allow for a selective coupling of the tetrazole-functionalized NBRs with the small molecular linker **5**. In the present study, a tetrazole was thus chosen exhibiting a cylization reactivity sufficiently low to not proceed with the double bonds of the NBR backbone, yet sufficiently high to proceed to high conversion within a reasonable time frame when adding the maleimide linker **5**.

Orthogonality of the nitrile imine to the double bonds of the polymer backbone was proven experimentally in a ^{1}H NMR model investigation (for ^{1}H NMR spectra, see Figure S1 in the Supporting Information). Solutions of tetrazole **3** in acetonitrile were irradiated with UV light at λ_{max} = 254 nm in the presence of 1-octene or *trans*-3-octene, chosen as model compounds mimicking the pendant and internal double bonds of the polymer backbone, respectively. While after irradiation in the presence of either 1-octene or *trans*-3-octene the absence of aromatic resonances of the diaryl tetrazole protons at 8.4 ppm

dx.doi.org/10.1021/ma401154k | Macromolecules XXXX, XXX, XXX−XXX

indicates a quantitative release of nitrogen, formation of the respective pyrazoline compounds is not observed and deactivation of the nitrile imine occurs via alternative pathways. In contrast, irradiation of **3** in the presence of maleimide quantitatively gives the pyrazoline adduct, as characterized by multiplets at 5.2 and 4.9 ppm. When irradiating **3** in the presence of both, *trans*-3-octene and maleimide, sole formation of the maleimide cycloadduct was observed. In 1,3-dipolar cycloaddition reactions of type I (according to Sustmann's classification[57]) the reaction rate of the cycloaddition reaction increases with a decrease in the free-energy gap between the highest occupied molecular orbital (HOMO) of the enophile and the lowest unoccupied molecular orbital (LUMO) of the dipolarophile.[58] Lin and co-workers were able to exploit the interrelation of the reaction rate and the free-energy gap by lifting the HOMO energy levels of the intermediate diaryl nitrile imines to reduce reaction times by tuning the aryl substitution pattern.[44] In analogy, the selectivity of the 1,3-dipolar cycloaddition toward maleimide observed in our study can be explained by the molecular orbital (MO) energy levels of the reactants. The LUMO energy levels of 1-octene, *trans*-3-octene and maleimide were accessed by DFT calculations and are reported in Table 1, entries 2−4. When comparing the LUMO energy levels of the olefins with the HOMO energy level of the nitrile imine intermediate of diaryl tetrazole **3′** (Table 1, entry 1), the free-energy gap between the MOs of the dipole and the dipolarophile increases in the order of maleimide < 1-octene < *trans*-3-octene, in line with the high reactivity observed for maleimide. To keep computational costs low, the HOMO energy level of the nitrile imine intermediate of tetrazole **3′** (see Figure S2) instead of **3** was used for discussion, since due to the distance of the trithiocarbonate and the ester moiety to the diaryl tetrazole moiety in compound **3**, the dissimilar substitution pattern will not have a pronounced effect on the obtained energy levels. The difference of the HOMO energy level of the nitrile imine intermediate of tetrazole **3′** obtained in the current study and the energy level earlier reported by Wang et al.,[44] is a result of the difference in the model chemistries (HF/3-21G//AM1 vs B3LYP/6-31G//B3LYP/6-31G) used. The LUMO energy level of the nitrile moiety—a potential 'ene' present in both the solvent and the NBR backbone—is positioned above the one of 1-octene. Nevertheless, light-induced coupling of tetrazole functional polymers with acetonitrile was observed when a plain solution of tetrazole functional polymer was irradiated with UV (see Figures S3 and S4) and can be explained with the high excess of solvent molecules relative to the polymer.

Table 1. Molecular Orbital Energies of the Dipole and the Dipolarophile Model Compounds[a]

entry	compound	E_{HOMO} (eV)	E_{LUMO} (eV)
1[b]	**3′**	−5.249	–
2	maleimide	–	−2.996
3	1-octene	–	0.659
4	*trans*-3-octene	–	0.727
5	acetonitrile	–	0.947

[a]Energies of the molecular orbitals are obtained via DFT calculations (B3LYP/6-31G//B3LYP/6-31G) and are given as zero-point corrected values. [b]The HOMO energy level of the nitrile imine intermediate of tetrazole **3′** is reported. The chemical structure of **3′** is provided in Figure S2.

A high density of the chain-end functionality of polymers is a prerequisite for effective orthogonal ligation reactions on polymers. When orthogonal to the polymerization process, the utilization of functionalized chain transfer agents in RAFT polymerizations allows for the synthesis of chain-end-functionalized polymers with a high functional density without the need for postpolymerization modifications.[8] Because of a low propagation rate coefficient,[59] the solution based reversible-deactivation radical copolymerization of AN and BD requires elevated temperatures to obtain moderate conversions. The thermal stability of **3** in solution was evidenced by comparison of the ^{1}H NMR spectra before and after heating the diaryl tetrazole at 100 °C for 8 h in DMSO-d_6 (Figure S5), allowing the direct synthesis of tetrazole functional polymers via the RAFT technique. The trithiocarbonate **3** was thus investigated toward its ability to control the free radical copolymerization of AN and BD. Polymerizations were performed at 100 °C in the absence of light. The obtained polymers **4a**−**4f** range from oligomeric species to polymers with molar masses of up to 38 000 g·mol^{-1}, while dispersities below 1.5 were observed. A slightly higher dispersity of 1.6 is observed for NBR **4f** of much higher molecular weight as a result of the prolonged reaction time and the therewith associated accumulation of inactive polymer chains. Experimental details for each individual polymerization are provided in Table 2. Molecular weights in the current study are reported as actual molar masses obtained from SEC via universal calibration employing the Mark−Houwink−Kuhn−Sakurada (MHKS) parameters of NBR,[53] recently determined by us. When comparing the molar masses obtained in the current study with those obtained under identical polymerization conditions reported in previous studies

Table 2. Experimental Details of the RAFT-Mediated Copolymerizations of AN/BD[a]

entry	RAFT agent	$[RAFT]_0$ (mM)	$[Ini]_0$ (mM)	t (h)	p^b (%)		M_n (g·mol^{-1})[c]	$Đ^c$
1[d]	**3**	91.1	5.5	3	37.2	**4a**	700[f]	1.2
2[e]	**3**	27.9	1.7	5.5	18.5	**4b**	1800	1.2
3	**3**	21.0	2.6	5	18.0	**4c**	3100	1.3
4	**3**	8.4	1.0	7	12.0	**4d**	4700	1.4
5	**3**	3.5	0.3	8	10.8	**4e**	9400	1.5
6	**3**	0.8	0.2	22	8.9	**4f**	38 000	1.6

[a]Conditions: NBR was synthesized with an overall monomer concentration of 9.5 mol·L^{-1} in chlorobenzene at 100 °C employing 1,1′-azobis(cyclohexane-1-carbonitrile) as a thermal initiator. Polymers were recovered by precipitation in ethanol, except otherwise stated. [b]Conversion was determined gravimetrically. [c]Obtained from SEC via universal calibration employing the MHKS parameters of NBR.[53] [d]Polymerization was performed in acetone; polymer was recovered by solvent evaporation. [e]Polymer was recovered by precipitation of polymer in cold hexane/Et_2O. [f]As a result of the low molecular weight, a strong deviation of molar mass obtained via universal calibration from the effective molar mass is observed. ESI-MS of polymer **4a** shows signals with the highest intensities at around 1100 Da.

dx.doi.org/10.1021/ma401154k | *Macromolecules* XXXX, XXX, XXX−XXX

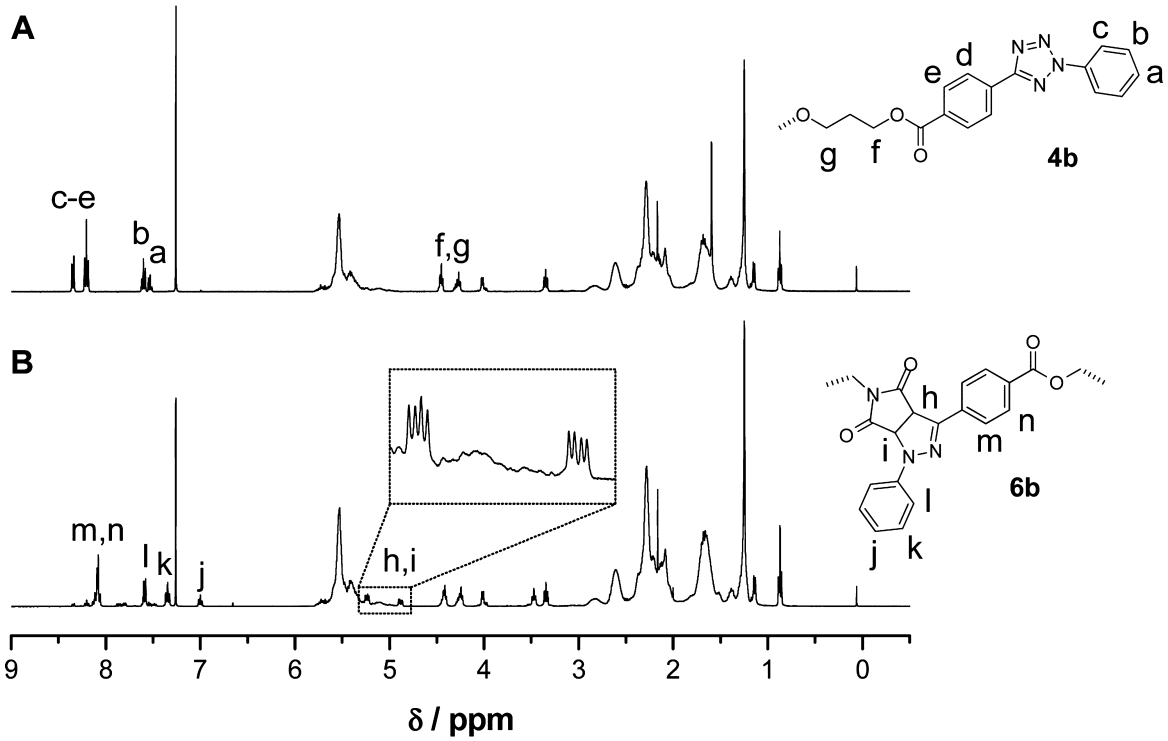

Figure 1. ^{1}H NMR characterization of (A) tetrazole-functionalized NBR **4b** of 1800 g·mol^{-1} and B) coupled NBR **6b** of 3200 g·mol^{-1}, both measured in $CDCl_3$.

a decrease by a factor of 2 in the values is observed. The decrease is a result of the higher K value of NBR relative to polystyrene (49.5×10^{-5} dL·g^{-1} vs 14.1×10^{-5} dL·g^{-1}), since tha α values are almost identical for NBR and polystyrene (0.689 vs 0.70).[60]

In the copolymerizations employing the photoreactive trithiocarbonate **3**, a linear relation of molar mass with conversion is observed as depicted in Figure S6, indicating living characteristics. The deviation from the linear behavior at the early polymerization stages is due to a hybrid effect as previously described.[61] The high end-group functionality of the obtained polymers **4** was proven by SEC-ESI mass spectrometry analysis. A magnified view into the region of 700 to 1400 Da of the low molecular weight NBR **4a** is provided in Figure S7 in the Supporting Information section. The main signals are assigned to the sodium adducts $[\mathbf{4}_{m+n} + Na]^+$ of the tetrazole-functional RAFT polymer, indicating formation of tetrazole-functionalized chains. Nevertheless, a small fraction of NBR **7** free of tetrazole functionality and unable to undergo further ligation is observed. These species are formed by the recombination of two propagating copolymer chains that were both initiated by the azo initiator fragment and are an inevitable side product of the RAFT process.[9] The observed signal pattern (see inset, Figure S7) is a result of the masses of the BD and AN repeat units differing in 1 Da only. Each individual signal can be assigned to the superposition of the isotope pattern of polymer chains with a similar degree of polymerization, DP = m + n, yet different ratios of the AN to BD contents, m/n. ^{1}H NMR analysis of the tetrazole-functionalized NBR **4b** is provided in Figure 1A and further confirms the formation of functionalized chains. The multiplet resonances between 8.4 and 7.1 ppm are assigned to the aromatic diaryl tetrazole chain-end protons a−e of the polymer. Moreover, the signals of the methylene protons in α-position to the ester moieties of the propyl linkage, f−g, are located at 4.4 and 4.2 ppm, respectively. Resonances at 0.9, 1.2, and 3.3 ppm indicate the presence of the Z-group dodecyl mercaptan chain-end as described in more detail for tetrazole functional NBR **4a** in Figure S8 in the Supporting Information. Identical chain-end resonances are observed when analyzing polymers of higher molecular weight.

In previous studies on photo-induced tetrazole−ene coupling, irradiation of tetrazoles to induce nitrogen release was performed at wavelengths ranging from 254 to 365 nm.[35−38,40−47] To choose an appropriate irradiation wavelength for our experiments, a UV absorption spectrum of the tetrazole functional chain transfer agent **3** was recorded. As depicted in Figure S9, the UV absorption spectrum of RAFT agent **3** (solid line) features a broad absorption band exhibiting its maximum absorption at 286 nm and is similar to the UV absorption spectrum of tetrazole functional NBR, exemplarily provided for NBR **4a** (dashed line). Nevertheless, the absorption of **3** (and **4**) is the result of the superposition of the absorption profiles of both, the tetrazole R-group and the trithiocarbonate chain-end. Contributions of the two individual components were investigated with model compounds possessing either the trithiocarbonate or the diaryl tetrazole feature. The latter is represented by 3-hydroxypropyl 4-(2-phenyl-2*H*-tetrazol-5-yl)benzoate (**9**, see Figure S10), obtained from tetrazole **2** by esterification with 1,3-propanediol, and exhibits an absorption maximum of 275 nm (dotted line). The esterified compound was used instead of **2** to preclude a batho- or hypsochrome influence of the carboxylate on the light absorption properties of the chromophore. Absorption of the trithiocarbonate is represented by ethyl 2-(((dodecylthio)carbonothioyl)thio)-propanoate (**8**, see Figure S10). The compound possesses a propanoate ester moiety and a dodecyl chain in vicinity to the trithiocarbonate—identical to the direct environment of the

dx.doi.org/10.1021/ma401154k | *Macromolecules* XXXX, XXX, XXX−XXX

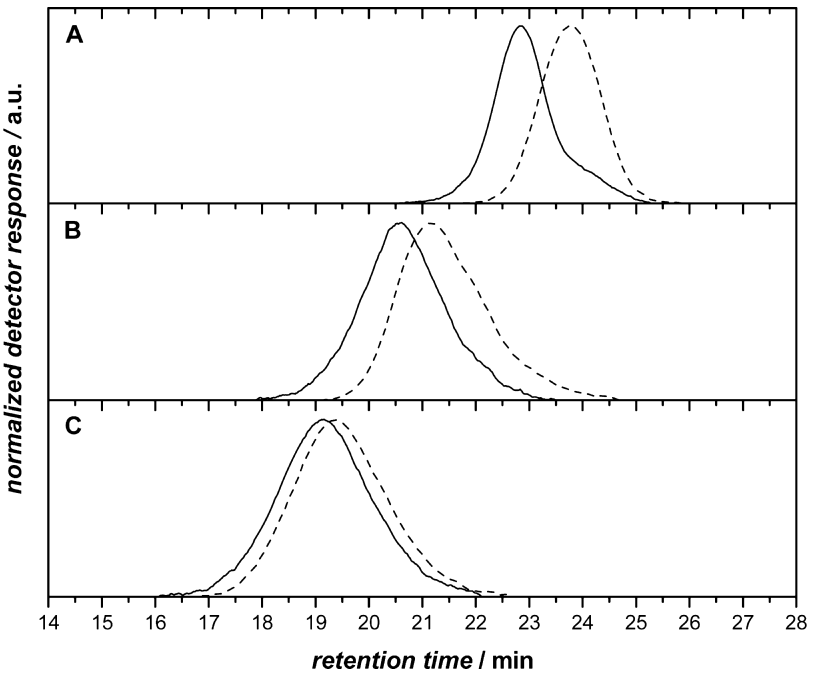

Figure 2. SEC traces of NBR coupling via the NITEC approach. SEC traces of coupled NBRs **6** are represented by solid lines, traces of tetrazole functional polymers **4** are depicted as dashed lines. (A) Coupling of NBR **4b** of 1800 g·mol^{-1} giving NBR **6b** of 3200 g·mol^{-1}, (B) coupling of NBR **4e** of 9400 g·mol^{-1} giving NBR **6e** of 17 000 g·mol^{-1}, and (C) coupling of NBR **4f** of 38 000 g·mol^{-1} giving NBR **6f** of 48 000 g·mol^{-1}. SEC data was evaluated employing the MHKS parameters of NBR.[53]

trithiocarbonate of controlling agent **3**—and shows its maximum absorption at 305 nm assigned to the $\pi-\pi^*$ transition of the trithiocarbonate (dash-dotted line). The polymerization via the RAFT process leads to an alteration of the direct environment of the trithiocarbonate, since the incorporation of monomers occurs in between the sulfur and the tertiary propanoate carbon after homolytic dissociation of the C−S single bond. Skrabania et al. reported a strong influence of the substitution patterns on the $\pi-\pi^*$ and n$-\pi^*$ transition of trithocarbonates.[62,63] Nevertheless, since **3** and **4a** do not show a significant disparity in their absorption, insights obtained from the trithiocarbonate **8** can be used to describe the absorption of the tetrazole-functionalized polymers **4a−f**. Supported by these results, in the current work nitrogen release from the tetrazoles to allow ligation of the nitrile rubbers is triggered by irradiation with a UV source of λ_{max} = 254 nm to facilitate absorption of the tetrazole while minimizing the interference with the trithiocarbonate.

The behavior of trithiocarbonate RAFT agents under UV irradiation has been subject to intensive investigations. Driven by the search for UV initiated controlled polymerization strategies, the radical decomposition pathways of trithiocarbonates have been elucidated.[64−66] In line with these experiments, the irradiation of trithiocarbonate **8** with UV light of 254 nm leads to a complete decomposition within 3 h. As depicted in Figure S11, the decomposition is evidenced in ^{1}H NMR spectroscopy by the loss of the propanoate methin and methyl proton resonances c and d at 4.8 and 1.6 ppm, respectively. Nevertheless, the UV induced coupling of the pure controlling agent **3** upon addition of 0.5 equiv of 5 quantitatively gave the respective pyrazoline **10** within 15 min without observing any decomposition of the trithiocarbonate. Formation of **10** is evidenced via ^{1}H NMR spectroscopy by the formation of multiplets of the methin protons d and e in α-position to the imide carbonyls, resonating at 5.2 and 4.9 ppm (Figure S12−S13). The conjugation further induces a shifting of the aromatic resonances a−c and f in comparison to those of tetrazole **3**. Moreover, resonances of the propanoate protons k and j in vicinity to the trithiocarbonate indicate that coupling is complete before decomposition of the trithiocarbonate occurs. However, prolonged irradiation is resulting in photobleaching of **10**. ^{1}H NMR spectra after irradiation of **3** in the presence of linker **5** for 15, 60, and 180 min is provided in Figure S14. While pure **10** is obtained after 15 and 60 min of irradiation, several aromatic signals are observed after 180 min of irradiation and indicate a decomposition of the pyrazoline coupling moiety.

In analogy to the UV-induced coupling of tetrazole functional controlling agent **3** giving the model compound **10**, NBRs **4** were subjected to UV irradiation in the presence of 0.5 equiv of linker **5**. In contrast to the small molecule couplings described above, a prolonged irradiation time of 180 min was necessary to obtain the coupled polymers. The necessity of prolonged reaction time is hypothesized to be caused by a deceleration of the cyclization step of the *in situ* formed nitrile imine and the maleimide. Cyclization of the polymeric nitrile imine with the maleimide is diffusion controlled and determines reaction rates, since polymer unfolding and the convergence of the nitrile imine and the maleimide functionality is a prerequisite for the cyclization. In contrast, the UV-induced nitrogen release does not require the vicinity of the reactants and therefore may not exhibit a dependency on the dimension of the reactants.

The SEC traces of the tetrazole-functionalized NBR precursors before and after the UV induced ligation are depicted in Figure 2. Traces of the coupled NBRs **6** (solid lines) exhibit a distinct shift to lower retention time and thus higher molecular weight when compared to those of the respective tetrazole-functionalized NBRs **4** (dashed lines). The SEC traces of the coupling of NBR **4b** is provided in Figure 2A.

dx.doi.org/10.1021/ma401154k | *Macromolecules* XXXX, XXX, XXX−XXX

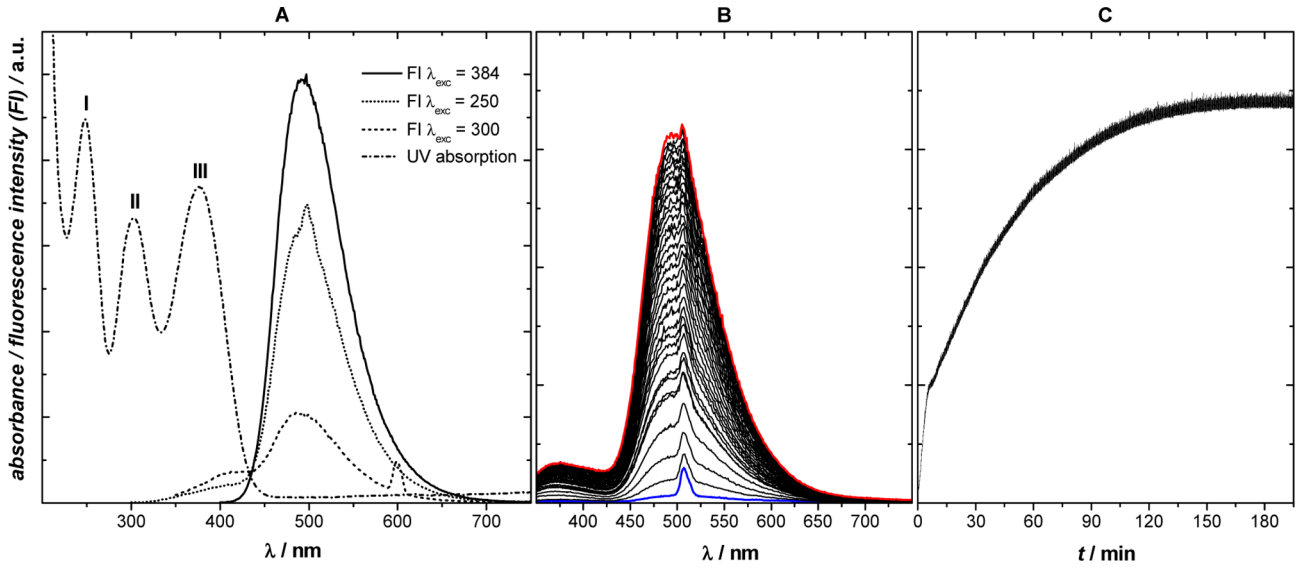

Figure 3. (A) Illustration of the UV absorption spectrum (dash-dotted line) and the fluorescence emission spectra at λ_{exc} of 254 nm (dotted line), 300 nm (dashed line) and 384 nm (solid line) of the model compound **10** coupled via NITEC. (B) Fluorescence emission spectra at λ_{exc} of 254 nm of tetrazole functional polymer **4d** in presence of 0.5 equiv of linker **5** measured at various irradiation times between the mixing of the starting materials (blue line) and 70 min of irradiation (red line). (C) Evolution of the FI with irradiation time at an emission wavelength λ_{em} of 497 nm and an excitation wavelength λ_{exc} of 254 nm.

The peak retention time shifts from 23.8 to 22.8 min and accounts for an increase of the molar mass from 1800 g·mol^{-1} to 3200 g·mol^{-1} (for details see Table S2, entry 1). The discrepancy of the theoretically expected molar mass M_n^{exp}(**6b**) of 3900 g·mol^{-1} (calculated from the sum of 2 × M_n(**4b**) + M(**5**)) and the experimentally observed molar mass can in part be explained with the commonly observed inaccuracy of molar masses in the low molecular weight region when calculated via universal calibration.[67] Nevertheless, the monomodal distribution of **6b** exhibits a slight tailing on the low molecular weight side. The tailing is a result of the presence of the nonfunctionalized polymer chains **7** unable to undergo conjugation.

Coupling of NBR **4e** of 9400 g·mol^{-1}, depicted in Figure 2B provides NBR **6e** of 17 000 g·mol^{-1} (Table S2, entry 2). Irradiation of NBR **4f** in the presence of **5** yields coupled NBR **6f** of 48 000 g·mol^{-1} (Figure 2C), exhibiting a dispersitiy of 1.6 (Table S2, entry 3). In analogy to the coupling of **4b** and **4e**, here a decrease in dispersity is not observed during conjugation. Since polymer coupling is a convolution procedure, in an ideal ligation reaction a doubling of molar mass along with a decrease in dispersity is expected.[68] However, simulations of RAFT-mediated copolymerizations of AN and BD theoretically confirmed the formation of up to 7 weight-% of nonfunctionalized polymers during polymerization.[50] These polymer species do not possess the targeted RAFT R-group functionality and lead to molar masses of the coupled polymers below the theoretically expected values, even in cases where a full conversion of the functional chain-ends occurs. As a consequence, a broadening of the molecular weight distributions is observed when nonfunctionalized polymer species are present in polymer−polymer coupling reactions.

Since the NITEC is a pro-fluorescent reaction, fluorescence spectroscopy allows the investigation of the polymer coupling reactions. A UV−vis absorption spectrum of the fluorescent model compound **10** is provided in Figure 3A as a dashed-dotted line and reveals the presence of three local absorption maxima around 250 nm (I), 300 nm (II), and 380 nm (III). The fluorescence emission spectra of **10** exhibit increasing relative fluorescence intensities (FI) at excitation wavelengths λ_{exc} of 250 nm (dotted line), 300 nm (dashed line) and 384 nm (solid line) in the order of II < I < III and allow the assignment of the absorption maxima I and III to the fluorescent chromophore. Absorption at 300 nm is caused by the trithiocarbonate moiety yet the occurrence of fluorescence most probably arises from the spectral overlap with absorption bands I and III. The feature at 500 nm observed in the emission spectrum at a λ_{exc} of 250 nm is a result of higher order transmissions.[69] Fluorescence emission spectra of the coupled NBRs **6** (not shown) exhibit features identical to **10**, proving the diaryl pyrazolines to be the moiety responsible for polymer−polymer coupling. The coincidence of the absorption wavelength of the fluorescent chromophore moiety with the wavelength employed for inducing the tetrazole−ene coupling of NBR building blocks, allows an *in situ* tracking of the cyclization progress with common fluorescence spectrometer equipment. Figure 3B shows the evolution of the fluorescence emission of a 28 μM solution of polymer **4d** in acetonitrile in the presence of 0.5 equiv of the maleimide linker **5** over the first 70 min of the reaction, excited with a λ_{exc} of 254 nm. A steady increase of the FI is observed, yet the increase slows down with the progress of the reaction. A plot of the FI of the emission spectra at an emission wavelength λ_{em} of 497 nm versus time, provided in Figure 3C, illustrates the plateauing of the FI at approximately 150 min of irradiation time. The time-dependent tracking of the reaction progress clearly evidence the necessity to perform the irradiation of polymeric tetrazoles on a longer time scale than required for small molecular analogues.

^{1}H NMR spectroscopy of coupled polymer **6b** is provided exemplarily in Figure 1B and exhibits resonances of the pyrazoline methin protons h and i in α-position to the carbonyls of the imide, resonating at 5.2 and 4.9 ppm and in part overlapping with resonances of the NBR backbone olefins (see inset). In analogy to the small molecule studies,

dx.doi.org/10.1021/ma401154k | *Macromolecules* XXXX, XXX, XXX−XXX

transformation of the diaryl tetrazole **4b** into the pyrazoline structure of **6b** induces a shift of the protons of the aryl substituents from 8.3, 8.2, 7.6, and 7.5 ppm (observed in the spectrum of the tetrazole functional polymer **4b**, Figure 1A, signals a−e) to 8.1, 7.6, 7.3, and 7.0 ppm (Figure 1B, signals j−n). Full conversion of the tetrazole functional chain-ends is evidenced by the absence of the resonances a−e in the spectrum of the coupled NBR **6b**. The small resonances in the aromatic region are traced back to bleaching effects as described for the conjugation model reaction of tetrazole functional controlling agent **3** (*vide supra*). The measurements confirm that the ligation of the tetrazole-functional NBRs exclusively occurs with the reactive maleimide linker, without attacking olefins within the polymer backbone.

CONCLUSION

In conclusion, the nitrile imine mediated tetrazole−ene coupling was demonstrated to be a fast and efficient method for the coupling of industrially relevant NBR building blocks to obtain nitrile rubber of high molecular weight. The method provided is an extraordinarily pure example of NBR conjugation since it is free of catalysts, additives or chemical stimuli and a postpolymerization transformation of the preformed polymer building blocks is not required prior to ligation. An appropriate choice of the dipolarophile linker and the nitrile imine precursor allowed the NITEC reaction to selectively proceed with the olefin linker. A reaction of the *in situ* formed enophile with the double bonds or the nitrile moieties of the incorporated monomer units within the polymer backbone—present in high excess relative to the dipolarophile linker molecule—was not observed. Underpinned by DFT calculations, the selectivity was explained by the reduced LUMO energy level of the maleimide linker compared to the nonactivated backbone olefins when employing a nitrile imine of moderate reactivity. An in-depth analysis of the coupled polymers revealed the maleimide derived fluorescent pyrazoline to be the element responsible for polymer−polymer coupling. The presented method is not limited to the coupling of linear NBR chains. By alteration of the architecture of the maleimide, block and starpolymers and polymer brushes can be accessed. In addition, the molecular weight, crucial for the performance of rubber products, may be further increased by utilizing α,ω-tetrazole bisfunctional NBR building blocks in a photo-induced step-growth polymerization process. Moreover, the modification of surfaces with maleimide might allow for the immobilization of NBR on solids opening up a wide field of technical applications.

ASSOCIATED CONTENT

Supporting Information

Experimental details, experimental procedures for the synthesis of **8**, NMR, SEC, UV−vis, and SEC−ESI−MS data. This material is available free of charge via the Internet at http://pubs.acs.org.

AUTHOR INFORMATION

Corresponding Author

*(C.B.K.) Fax: +49 721 608 45740. E-mail: christopher.barner-kowollik@kit.edu.

Notes

The authors declare no competing financial interest.

ACKNOWLEDGMENTS

The authors thank Lanxess Deutschland GmbH for supporting the current project and the excellent collaboration. C.B.-K. acknowledges additional funding from the Karlsruhe Institute of Technology (KIT) via its Excellence and Helmholtz programs as well as the German Research Council (DFG) and the Ministry of Arts and Science of the State of Baden-Württemberg via their large equipment schemes. The authors thank Astrid Hirschbiel (KIT) for measuring the SEC ESI−MS spectra. Lukas Stolzer (KIT) is acknowledged for his help with the fluorescence measurements, while we are grateful to Dr. Thomas Wolf (KIT) for useful discussions reagarding the DFT calculations.

ABBREVIATIONS

AN, Acrylonitrile; BD, 1,3-butadiene; NITEC, nitrile imine mediated tetrazole−ene coupling; NBR, nitrile−butadiene rubber; RAFT, reversible addition−fragmentation chain transfer; FI, fluorescene intensity

REFERENCES

(1) Becer, C. R.; Hoogenboom, R.; Schubert, U. S. *Angew. Chem., Int. Ed.* **2009**, *48* (27), 4900−4908.
(2) Iha, R. K.; Wooley, K. L.; Nyström, A. M.; Burke, D. J.; Kade, M. J.; Hawker, C. J. *Chem. Rev.* **2009**, *109* (11), 5620−−5686.
(3) Barner-Kowollik, C.; Du Prez, F. E.; Espeel, P.; Hawker, C. J.; Junkers, T.; Schlaad, H.; Van Camp, W. *Angew. Chem., Int. Ed.* **2011**, *50* (1), 60−62.
(4) Hawker, C. J.; Wooley, K. L. *Science* **2005**, *309* (5738), 1200−1205.
(5) Solomon, D. H.; Rizzardo, E.; Cacioli, P. *Polymerization Process and Polymers Produced Thereby*. US 4,581,429, April 8, 1986.
(6) Wang, J.-S.; Matyjaszewski, K. *J. Am. Chem. Soc.* **1995**, *117* (20), 5614−5615.
(7) Chiefari, J.; Chong, Y. K.; Ercole, F.; Krstina, J.; Jeffery, J.; Le, T. P. T.; Mayadunne, R. T. A.; Meijs, G. F.; Moad, C. L.; Moad, G.; Rizzardo, E.; Thang, S. H. *Macromolecules* **1998**, *31* (16), 5559−5562.
(8) Barner-Kowollik, C., *Handbook of RAFT Polymerization*; Wiley-VCH: Weinheim, Germany, 2009.
(9) Moad, G.; Rizzardo, E.; Thang, S. H. *Aust. J. Chem.* **2005**, *58* (6), 379−410.
(10) Moad, G.; Rizzardo, E.; Thang, S. H. *Aust. J. Chem.* **2006**, *59* (10), 669−692.
(11) Moad, G.; Rizzardo, E.; Thang, S. H. *Aust. J. Chem.* **2009**, *62* (11), 1402−1472.
(12) Moad, G.; Rizzardo, E.; Thang, S. H. *Aust. J. Chem.* **2012**, *65* (8), 985−1076.
(13) Braunecker, W. A.; Matyjaszewski, K. *Prog. Polym. Sci.* **2007**, *32* (1), 93−146.
(14) Sumerlin, B. S.; Vogt, A. P. *Macromolecules* **2010**, *43* (1), 1−13.
(15) Wu, P.; Feldman, A. K.; Nugent, A. K.; Hawker, C. J.; Scheel, A.; Voit, B.; Pyun, J.; Fréchet, J. M. J.; Sharpless, K. B.; Fokin, V. V. *Angew. Chem., Int. Ed.* **2004**, *43* (30), 3928−3932.
(16) Franc, G.; Kakkar, A. K. *Chem. Soc. Rev.* **2010**, *39* (5), 1536−1544.
(17) Altintas, O.; Vogt, A. P.; Barner-Kowollik, C.; Tunca, U. *Polym. Chem.* **2012**, *3* (1), 34−45.
(18) Ranjan, R.; Brittain, W. J. *Macromolecules* **2007**, *40* (17), 6217−6223.
(19) Goldmann, A. S.; Tischer, T.; Barner, L.; Bruns, M.; Barner-Kowollik, C. *Biomacromolecules* **2011**, *12* (4), 1137−1145.
(20) Kolb, H. C.; Finn, M. G.; Sharpless, K. B. *Angew. Chem., Int. Ed.* **2001**, *40* (11), 2004−2021.
(21) Yamada, Y. M. A.; Sarkar, S. M.; Uozumi, Y. *J. Am. Chem. Soc.* **2012**, *134* (22), 9285−9290.

(22) Boren, B. C.; Narayan, S.; Rasmussen, L. K.; Zhang, L.; Zhao, H.; Lin, Z.; Jia, G.; Fokin, V. V. *J. Am. Chem. Soc.* **2008**, *130* (28), 8923−8930.
(23) Agard, N. J.; Prescher, J. A.; Bertozzi, C. R. *J. Am. Chem. Soc.* **2004**, *126* (46), 15046−15047.
(24) Tasdelen, M. A. *Polym. Chem.* **2011**, *2*, 2133−2145.
(25) Gody, G.; Rossner, C.; Moraes, J.; Vana, P.; Maschmeyer, T.; Perrier, S. *J. Am. Chem. Soc.* **2012**, *134* (30), 12596−12603.
(26) He, Y.; He, W.; Liu, D.; Gu, T.; Wei, R.; Wang, X. *Polym. Chem.* **2013**, *4* (2), 402−406.
(27) Heredia, K. L.; Tolstyka, Z. P.; Maynard, H. D. *Macromolecules* **2007**, *40* (14), 4772−4779.
(28) Blackman, M. L.; Royzen, M.; Fox, J. M. *J. Am. Chem. Soc.* **2008**, *130* (41), 13518−13519.
(29) Singh, I.; Zarafshani, Z.; Lutz, J.-F. o.; Heaney, F. *Macromolecules* **2009**, *42* (15), 5411−5413.
(30) Pauloehrl, T.; Delaittre, G.; Bruns, M.; Meißler, M.; Börner, H. G.; Bastmeyer, M.; Barner-Kowollik, C. *Angew. Chem., Int. Ed.* **2012**, *51* (36), 9181−9184.
(31) Delaittre, G.; Pauloehrl, T.; Bastmeyer, M.; Barner-Kowollik, C. *Macromolecules* **2012**, *45* (4), 1792−1802.
(32) Pauloehrl, T.; Delaittre, G.; Winkler, V.; Welle, A.; Bruns, M.; Börner, H. G.; Greiner, A. M.; Bastmeyer, M.; Barner-Kowollik, C. *Angew. Chem., Int. Ed.* **2012**, *51* (4), 1071−1074.
(33) Pauloehrl, T.; Delaittre, G.; Bastmeyer, M.; Barner-Kowollik, C. *Polym. Chem.* **2012**, *3* (7), 1740−1749.
(34) Poloukhtine, A. A.; Mbua, N. E.; Wolfert, M. A.; Boons, G.-J.; Popik, V. V. *J. Am. Chem. Soc.* **2009**, *131* (43), 15769−15776.
(35) Song, W.; Wang, Y.; Qu, J.; Madden, M. M.; Lin, Q. *Angew. Chem., Int. Ed.* **2008**, *47* (15), 2832−2835.
(36) Wang, Y.; Rivera Vera, C. I.; Lin, Q. *Org. Lett.* **2007**, *9* (21), 4155−4158.
(37) Wang, Y.; Hu, W. J.; Song, W.; Lim, R. K. V.; Lin, Q. *Org. Lett.* **2008**, *10* (17), 3725−3728.
(38) Yu, Z.; Ho, L. Y.; Wang, Z.; Lin, Q. *Bioorg. Med. Chem. Lett.* **2011**, *21* (17), 5033−5036.
(39) Clovis, J. S.; Eckell, A.; Huisgen, R.; Sustmann, R. *Chem. Ber.* **1967**, *100* (1), 60−70.
(40) Madden, M. M.; Rivera Vera, C. I.; Song, W.; Lin, Q. *Chem. Commun.* **2009**, *37*, 5588−5590.
(41) Song, W.; Wang, Y.; Yu, Z.; Rivera Vera, C. I.; Qu, J.; Lin, Q. *ACS Chem. Biol.* **2010**, *5* (9), 875−885.
(42) Yu, Z.; Lim, R. K. V.; Lin, Q. *Chem.—Eur. J.* **2010**, *16* (45), 13325−13329.
(43) Wang, J.; Zhang, W.; Song, W.; Wang, Y.; Yu, Z.; Li, J.; Wu, M.; Wang, L.; Zang, J.; Lin, Q. *J. Am. Chem. Soc.* **2010**, *132* (42), 14812−14818.
(44) Wang, Y.; Song, W.; Hu, W. J.; Lin, Q. *Angew. Chem., Int. Ed.* **2009**, *48* (29), 5330−5333.
(45) Song, W.; Wang, Y.; Qu, J.; Lin, Q. *J. Am. Chem. Soc.* **2008**, *130* (30), 9654−9655.
(46) de Hoog, H.-P. M.; Nallani, M.; Liedberg, B. *Polym. Chem.* **2012**, *3* (2), 302−306.
(47) Dietrich, M.; Delaittre, G.; Blinco, J. P.; Inglis, A. J.; Bruns, M.; Barner-Kowollik, C. *Adv. Funct. Mater.* **2012**, *22* (2), 304−312.
(48) Kaiser, A.; Brandau, S.; Klimpel, M.; Barner-Kowollik, C. *Macromol. Rapid Commun.* **2010**, *31* (18), 1616−1621.
(49) Dürr, C. J.; Emmerling, S. G. J.; Kaiser, A.; Brandau, S.; Habicht, A. K. T.; Klimpel, M.; Barner-Kowollik, C. *J. Polym. Sci., Part A: Polym. Chem.* **2012**, *50* (1), 174−180.
(50) Dürr, C. J.; Hlalele, L.; Kaiser, A.; Brandau, S.; Barner-Kowollik, C. *Macromolecules* **2013**, *46* (1), 49−62.
(51) Dürr, C. J.; Emmerling, S. G. J.; Lederhose, P.; Kaiser, A.; Brandau, S.; Klimpel, M.; Barner-Kowollik, C. *Polym. Chem.* **2012**, *3* (4), 1048−1060.
(52) Nagdi, K. *Gummi-Werkstoffe: ein Ratgeber für Anwender ; Arten - Zusammensetzung - Verarbeitung - Eigenschaften - Beständigkeiten - Anwendungen - Prüfungen - Qualitätskontrolle - Klassifizierung - Chemie*, 3rd ed.; Gupta: Ratingen, Germany, 2004; p 431.
(53) Dürr, C. J.; Hlalele, L.; Schneider-Baumann, M.; Kaiser, A.; Brandau, S.; Barner-Kowollik, C. *Polym. Chem.* **2013**, DOI: 10.1039/C3PY00580A.
(54) Gruendling, T.; Guilhaus, M.; Barner-Kowollik, C. *Anal. Chem.* **2008**, *80* (18), 6915−6927.
(55) Hertz, D. L.; Bussem, H.; Ray, T. W. *Rubber Chem. Technol.* **1995**, *68* (3), 540−546.
(56) Stille, J. K.; Chen, A. T. *Macromolecules* **1972**, *5* (4), 377−384.
(57) Sustmann, R. *Tetrahedron Lett.* **1971**, *12* (29), 2717−2720.
(58) Houk, K. N.; Sims, J.; Watts, C. R.; Luskus, L. J. *J. Am. Chem. Soc.* **1973**, *95* (22), 7301−7315.
(59) Hlalele, L.; Dürr, C. J.; Lederhose, P.; Kaiser, A.; Hüsgen, S.; Brandau, S.; Barner-Kowollik, C. *Macromolecules* **2013**, *46* (6), 2109−2117.
(60) Strazielle, C.; Benoit, H.; Vogl, O. *Eur. Polym. J.* **1978**, *14* (5), 331−334.
(61) Barner-Kowollik, C.; Quinn, J. F.; Nguyen, T. L. U.; Heuts, J. P. A.; Davis, T. P. *Macromolecules* **2001**, *34* (22), 7849−7857.
(62) Skrabania, K. *The multifarious self-assembly of triblock copolymers: from multi-responsive polymers and multi-compartment micelles*. Ph.D. Thesis, University of Potsdam: 2008.
(63) Skrabania, K.; Miasnikova, A.; Bivigou-Koumba, A. M.; Zehm, D.; Laschewsky, A. *Polym. Chem.* **2011**, *2* (9), 2074−2083.
(64) Quinn, J. F.; Barner, L.; Barner-Kowollik, C.; Rizzardo, E.; Davis, T. P. *Macromolecules* **2002**, *35* (20), 7620−7627.
(65) Lu, L.; Zhang, H.; Yang, N.; Cai, Y. *Macromolecules* **2006**, *39* (11), 3770−3776.
(66) You, Y.-Z.; Hong, C.-Y.; Bai, R.-K.; Pan, C.-Y.; Wang, J. *Macromol. Chem. Phys.* **2002**, *203* (3), 477−483.
(67) Chance, R. R.; Baniukiewicz, S. P.; Mintz, D.; Strate, G. V.; Hadjichristidis, N. *Int. J. Polym. Anal. Charact.* **1995**, *1* (1), 3−34.
(68) Barner-Kowollik, C. *Macromol. Rapid Commun.* **2009**, *30* (19), 1625−1631.
(69) Lakowicz, J. R. *Principles of fluorescence spectroscopy*; Springer: New York, 2009.